



ELSEVIER

SCIENCE @ DIRECT®

PHYSICS LETTERS B

Physics Letters B 594 (2004) 23–34

www.elsevier.com/locate/physletb

Closing the light sbottom mass window from a compilation of $e^+e^- \rightarrow$ hadron data

Patrick Janot

PH Department, CERN, CH-1211 Geneva 23, Switzerland

Received 7 April 2004; accepted 20 April 2004

Available online 4 June 2004

Editor: W.-D. Schlatter

Abstract

The $e^+e^- \rightarrow$ hadron cross section data from PEP, PETRA, TRISTAN, SLC and LEP, at centre-of-mass energies between 20 to 209 GeV, are analysed to search for the production of a pair of light sbottoms decaying hadronically via R-parity-violating couplings. This analysis allows the 95% C.L. exclusion of such a particle if its mass is below $7.5 \text{ GeV}/c^2$. The light sbottom mass window is closed.

© 2004 Elsevier B.V. Open access under [CC BY license](http://creativecommons.org/licenses/by/4.0/).

1. Introduction

At the end of the last millenium, the Tevatron Collaborations [1,2] came out with a bottom quark production cross section at $\sqrt{s} = 1.8 \text{ TeV}$ in excess of the theoretical prediction by about a factor of two. Refined parton density functions and other theoretical improvements, e.g., in the b-quark fragmentation function, have recently been shown to account for the difference in the data recorded at $\sqrt{s} = 1.96 \text{ TeV}$ [3].

A more exotic model [4], in which a pair of gluinos with mass 12 to 16 GeV/c^2 is produced in $p\bar{p}$ collisions, with subsequent decays into a bottom quark and a light sbottom, with mass below $6 \text{ GeV}/c^2$, has been shown to also fit the excess well. In this model, the sbottom must either be long-lived or decay via R-parity-violating coupling to light quarks,

e.g., $\tilde{b} \rightarrow \bar{u}s$, to comply with various experimental constraints. Long-lived sbottoms have recently been excluded up to masses of $92 \text{ GeV}/c^2$ by ALEPH [5] in direct searches for $e^+e^- \rightarrow q\bar{q}\tilde{q}\tilde{q}$ and $e^+e^- \rightarrow \tilde{q}\tilde{q}$, but R-parity-violating prompt hadronic decays have not been addressed by the ALEPH analysis.

A light, hadronically decaying sbottom would increase the $e^+e^- \rightarrow$ hadron cross section above the $\tilde{b}\tilde{b}$ production threshold by up to a quarter of the $e^+e^- \rightarrow b\bar{b}$ cross section, i.e., about 2% far from the Z peak and 5% at the Z peak. For this reason, the measurements of the hadronic cross section at centre-of-mass energies from 20 to 209 GeV (i.e., well above the known $b\bar{b}$ resonances) from PEP [6,7], PETRA [8–13], TRISTAN [14–20] and LEP and SLC [21], are reanalysed in this Letter to search for a possible consistent excess.

This Letter is organized as follows. A compilation of the data is presented in a synthetic manner in [Section 2](#) to allow easy reinterpretation in the future.

E-mail address: patrick.janot@cern.ch (P. Janot).

The global fit of the data is described in Section 3. The results of the analysis are given in Section 4 and the conclusions are listed in Section 5.

2. The hadronic cross section data

2.1. The data from PEP, PETRA and TRISTAN

Most of the data from PEP, PETRAN and TRISTAN are published under the form of the ratio R of the effective Born hadronic cross section σ_{had}^0 to the point-like $e^+e^- \rightarrow \mu^+\mu^-$ cross section $\sigma_{\mu\mu}^0$,

$$\sigma_{\mu\mu}^0(s) = \frac{\alpha_{\text{QED}}^2(s)}{\alpha_{\text{QED}}^2(0)} \times \frac{86.85 \text{ nb}}{s}, \quad (1)$$

where s is the e^+e^- centre-of-mass energy squared and α_{QED} is the fine structure constant. The latest TOPAZ [16,17] and VENUS [20] publications report directly the value of σ_{had}^0 instead. In both cases, the latter includes a correction that unfolds the effects of initial state radiation (ISR), while still reflecting the running of the fine structure constant with the centre-of-mass energy [22].

The R and σ_{had}^0 data are listed in Table 1 (PEP, PETRA) and in Table 2 (TRISTAN), as obtained from a comparison of two recent compilations [23, 24] and the original publications [6–20]. In these tables, only the final—and most accurate—result for each experiment and each centre-of-mass energy is reported. (Superseded data are reported in both Refs. [23,24], but are not always clearly flagged as such therein.)

Other refinements were considered in this Letter for a rigorous statistical treatment of the data, and are described in the following. First, in each experiment, the systematic uncertainty was divided into a point-to-point contribution, σ_{ptp} , and an overall normalization error, Δ_{norm} , as is done in most of the original publications. The point-to-point systematic uncertainties are uncorrelated (related to, e.g., the limited simulated statistics, or the statistical uncertainty on the measured luminosity), are assumed to have a Gaussian probability density function and are taken directly from the original publications.

In contrast, the overall normalization error definition varies among the publications, being either the

largest possible variation interval (e.g., between several sets of selection criteria, different ways of determining the luminosity, or various quark fragmentation models) or half this interval. Here, the definition was unified in such a way that the overall normalization can vary by $-\Delta_{\text{norm}}$ and $+\Delta_{\text{norm}}$, with a uniform probability over the whole interval. This overall normalization error is 100% correlated between the different centre-of-mass energy points reported in each given publication.

Third, the published values of Δ_{norm} often contain an estimate of the effect of missing higher-order QED corrections in the ISR unfolding procedure, at the level of a couple of percent. Indeed, at the time of PEP, PETRA and TRISTAN, the Monte Carlo programs used to simulate the $e^+e^- \rightarrow q\bar{q}$ and $e^+e^- \rightarrow e^+e^-$ processes were limited to $\mathcal{O}(\alpha_{\text{QED}})$. The missing orders have a potential effect on the measured value of σ_{had}^0 via the prediction of both the hadronic cross section and the Bhabha scattering cross section: the former is used to correct the measured σ_{had} for QED effects, and the latter to determine the integrated luminosity. Altogether, the published cross section values would have to be corrected as follows,

$$\sigma_{\text{had}}^0 \rightarrow \sigma_{\text{had}}^0 \times \frac{\sigma_{\text{ee}}^{(\text{all})}}{\sigma_{\text{ee}}^{(1)}} \frac{\sigma_{\text{had}}^{(1)}}{\sigma_{\text{had}}^{(\text{all})}}, \quad (2)$$

where the indices (1) and (all) refer to the cross section prediction up to the QED first order (used in the original publications) and with all orders, respectively.

With the programs that have been developed for LEP, it is now possible to evaluate this correction with a better accuracy than that assumed twenty years ago. The $e^+e^- \rightarrow q\bar{q}$ and $e^+e^- \rightarrow e^+e^-$ cross sections were determined here with and without QED higher orders by ZFITTER [25] with an emulation of the kinematical cuts described in the original publications. It was found that the corrections to Bhabha scattering and hadron production essentially cancel in the ratio of Eq. (2). The remaining contribution of QED higher orders is at the 0.1% level, almost independently of the event selection and the centre-of-mass energy.

The large uncertainties related to the missing QED higher orders were therefore taken out from the original values of Δ_{norm} . While the aforementioned 0.1% contribution could be simply corrected for in σ_{had}^0 , a new normalization error $\Delta_{\text{QED}} = 0.1\%$ was added in-

Table 1

The ratio R and the effective Born hadronic cross section, σ_{had}^0 , from the PEP and PETRA experiments, with increasing centre-of-mass energy (\sqrt{s}). The expected statistical (σ_{stat}), point-to-point systematic (σ_{ptp}) and normalization systematic (Δ_{norm}) uncertainties are also given (in %). The latter is correlated between all energy points in a given publication. An additional normalization error $\Delta_{\text{QED}} = 0.1\%$, fully correlated between all measurements, is to be added to account for missing QED higher orders. The last column points to the original publication

\sqrt{s} (GeV)	Ratio R	σ_{had}^0 (pb)	σ_{stat} (%)	σ_{ptp} (%)	Δ_{norm} (%)	Reference
21.990	3.550	697.0	2.4	3.0	1.6	MARK J [10]
22.000	3.860	757.2	3.0	2.1	1.7	CELLO [8]
21.990	3.860	757.9	2.3	0.0	3.5	TASSO [12]
22.000	4.110	806.2	3.1	0.0	2.4	JADE [9]
22.000	3.470	680.7	18.3	0.0	6.0	PLUTO [13]
25.000	3.720	566.7	10.4	0.0	3.5	TASSO [11]
25.000	4.030	613.9	5.1	3.0	1.6	MARK J [10]
25.010	4.240	645.4	6.5	0.0	2.4	JADE [9]
27.500	3.910	493.3	8.2	0.0	3.5	TASSO [11]
27.600	4.070	509.8	7.0	0.0	6.0	PLUTO [13]
27.660	3.850	480.2	12.5	0.0	2.4	JADE [9]
29.000	3.920	445.3	1.3	0.0	2.3	MARK II [6]
29.000	3.960	449.8	0.8	0.0	2.3	MAC [7]
29.930	3.550	378.8	11.8	0.0	2.4	JADE [9]
30.100	3.940	415.8	4.5	0.0	3.5	TASSO [11]
30.380	3.850	398.9	5.0	0.0	2.4	JADE [9]
30.610	4.150	423.6	3.5	3.0	1.6	MARK J [10]
30.800	4.100	413.4	3.1	0.0	6.0	PLUTO [13]
31.100	3.660	362.0	5.1	0.0	3.5	TASSO [11]
31.290	3.830	374.3	7.4	0.0	2.4	JADE [9]
33.200	4.090	355.5	4.5	0.0	3.5	TASSO [11]
33.790	3.860	324.1	1.8	3.0	1.6	MARK J [10]
33.800	3.740	313.8	2.7	1.9	1.7	CELLO [8]
33.890	4.160	347.2	2.3	0.0	2.4	JADE [9]
34.000	4.120	341.7	2.6	0.0	3.5	TASSO [11]
34.500	3.930	316.6	5.1	0.0	2.4	JADE [9]
34.610	3.780	302.6	0.8	3.0	1.6	MARK J [10]
34.700	4.080	325.0	2.2	0.0	3.5	TASSO [11]
35.000	4.150	325.0	0.5	0.0	3.5	TASSO [12]
35.010	3.930	307.6	2.5	0.0	2.4	JADE [9]
35.100	3.940	306.8	1.5	3.0	1.6	MARK J [10]
35.450	3.930	300.1	4.6	0.0	2.4	JADE [9]
36.100	3.930	289.5	4.8	0.0	3.5	TASSO [11]
36.310	3.880	282.5	4.2	3.0	1.6	MARK J [10]
36.380	3.710	269.1	5.8	0.0	2.4	JADE [9]
37.400	3.590	246.6	9.3	3.0	1.6	MARK J [10]
38.300	3.890	254.9	2.6	1.7	1.7	CELLO [8]
38.380	4.030	263.0	4.7	3.0	1.6	MARK J [10]
40.320	4.050	239.7	4.7	0.0	2.6	JADE [9]
40.340	3.870	228.9	4.2	3.0	1.6	MARK J [10]
41.180	4.210	239.0	5.1	0.0	2.6	JADE [9]
41.500	4.030	225.3	4.2	1.8	1.7	CELLO [8]
41.500	4.440	248.3	4.5	3.0	1.6	MARK J [10]
42.500	3.890	207.5	5.2	3.0	1.6	MARK J [10]
42.550	4.200	223.5	5.1	0.0	2.6	JADE [9]
43.460	3.750	191.4	4.7	3.0	1.6	MARK J [10]
43.500	3.970	202.2	2.0	1.4	1.7	CELLO [8]
43.530	4.000	203.5	5.0	0.0	2.6	JADE [9]
43.700	4.110	207.5	1.2	0.0	3.5	TASSO [12]
44.200	4.010	197.9	2.5	1.2	1.7	CELLO [8]
44.230	4.150	204.6	1.9	3.0	1.6	MARK J [10]
44.410	3.980	194.6	5.1	0.0	2.6	JADE [9]
45.480	4.170	194.5	4.5	3.0	1.6	MARK J [10]
45.590	4.400	204.3	4.8	0.0	2.6	JADE [9]
46.000	4.090	186.6	5.2	1.9	1.7	CELLO [8]
46.470	4.420	197.6	3.7	3.0	1.6	MARK J [10]
46.470	4.040	180.6	6.0	0.0	2.6	JADE [9]
46.600	4.200	186.7	8.5	1.7	1.7	CELLO [8]

Table 2

The ratio R and the effective Born hadronic cross section, σ_{had}^0 , from the TRISTAN experiments, with increasing centre-of-mass energy (\sqrt{s}). The expected statistical (σ_{stat}), point-to-point systematic (σ_{ptp}) and normalization systematic (Δ_{norm}) relative uncertainties are also given (in %). The latter is correlated between all energy points in a given publication. An additional normalization error $\Delta_{\text{QED}} = 0.1\%$, fully correlated between all measurements, is to be added to account for missing QED higher orders. The last column points to the original publication

\sqrt{s} (GeV)	Ratio R	σ_{had}^0 (pb)	σ_{stat} (%)	σ_{ptp} (%)	Δ_{norm} (%)	Reference
50.000	4.530	175.2	12.7	2.3	2.7	TOPAZ [15]
50.000	4.400	170.2	11.2	4.0	0.7	VENUS [18]
50.000	4.500	174.1	10.5	2.8	1.6	AMY [14]
52.000	4.530	162.1	4.6	1.1	2.7	TOPAZ [15]
52.000	4.700	168.2	6.2	4.0	0.7	VENUS [18]
52.000	4.289	153.5	4.7	2.2	1.6	AMY [14]
54.000	4.979	165.4	10.9	3.4	2.7	TOPAZ [15]
54.000	4.688	155.7	9.2	1.8	1.6	VENUS [19]
54.000	4.725	156.9	12.8	3.4	1.6	AMY [14]
55.000	4.639	148.6	5.4	1.4	2.7	TOPAZ [15]
55.000	4.317	138.3	7.2	1.8	1.6	VENUS [19]
55.000	4.632	148.4	5.2	1.4	1.6	AMY [14]
56.000	5.068	156.7	4.2	0.8	2.7	TOPAZ [15]
56.000	4.655	143.9	3.9	1.8	1.6	VENUS [19]
56.000	5.207	161.0	3.5	1.1	1.6	AMY [14]
56.500	5.108	155.2	9.1	2.1	2.7	TOPAZ [15]
56.500	3.935	119.5	11.5	1.8	1.6	VENUS [19]
56.500	5.324	161.7	8.7	2.5	1.6	AMY [14]
57.000	5.147	153.7	4.7	1.1	2.7	TOPAZ [15]
57.000	4.983	148.7	4.3	1.8	1.6	VENUS [19]
57.000	4.903	146.4	4.5	1.3	1.6	AMY [14]
57.370	4.432	130.6	10.4	0.0	2.2	TOPAZ [16]
57.770	4.878	141.8	0.9	0.9	0.0	VENUS [20]
57.770	4.940	143.6	1.0	0.0	2.2	TOPAZ [17]
57.970	4.832	139.5	9.4	0.0	2.2	TOPAZ [16]
58.220	4.727	135.3	9.1	0.0	2.2	TOPAZ [16]
58.290	5.336	152.4	8.0	1.7	2.7	TOPAZ [15]
58.470	4.291	121.8	10.7	0.0	2.2	TOPAZ [16]
58.500	4.909	139.2	8.9	1.8	1.6	VENUS [19]
58.500	5.303	150.4	10.4	2.0	1.6	AMY [14]
58.720	4.811	135.4	8.3	0.0	2.2	TOPAZ [16]
58.970	5.582	155.8	8.0	0.0	2.2	TOPAZ [16]
59.000	4.848	135.2	9.7	1.8	1.6	VENUS [19]
59.000	5.409	150.8	10.9	2.8	1.6	AMY [14]
59.050	6.055	168.5	9.8	1.8	1.6	VENUS [19]
59.050	6.582	183.2	10.8	2.6	1.6	AMY [14]
59.060	5.735	159.6	7.1	2.1	2.7	TOPAZ [15]
59.220	5.084	140.7	9.3	0.0	2.2	TOPAZ [16]
59.470	5.447	149.5	9.8	0.0	2.2	TOPAZ [16]
59.840	4.717	127.9	8.1	0.0	2.2	TOPAZ [16]
60.000	5.305	143.1	5.4	1.3	2.7	TOPAZ [15]
60.000	5.274	142.2	4.7	1.8	1.6	VENUS [19]
60.000	5.809	156.7	4.7	1.3	1.6	AMY [14]
60.800	5.653	148.5	4.8	1.1	2.7	TOPAZ [15]
60.800	5.680	149.2	4.1	1.8	1.6	VENUS [19]
60.800	5.544	145.7	5.2	1.9	1.6	AMY [14]
61.400	5.852	150.8	5.1	1.4	2.7	TOPAZ [15]
61.400	4.990	128.6	4.4	1.8	1.6	VENUS [19]
61.400	5.410	139.4	5.0	1.4	1.6	AMY [14]
63.600	6.126	147.2	10.7	1.8	1.6	VENUS [19]

stead (assumed to be 100% correlated between all PEP, PETRA and TRISTAN measurements) to conservatively account for the yet missing orders in ZFITTER.

Finally, early TRISTAN data [14,15,18,19] are also corrected in the original publications for other electroweak effects, dominated by the top quark contribution (with a $(m_{\text{top}}/m_Z)^2$ dependence at first order). These small corrections (between +0.1% and +0.7% at $\sqrt{s} = 60$ GeV, depending on the top quark mass chosen to determine the correction) were unfolded here (i) to have a consistent data set to work with; and (ii) for a sound comparison with the ZFITTER prediction, which includes first- and higher-order electroweak contributions as well. The latest TRISTAN data [16,17,20] were, more adequately, corrected for QED effects only. The electroweak effect correction needs therefore not be unfolded in that case.

For practical reasons, the measurements of Tables 1 and 2 were clustered in few centre-of-mass bins as indicated by the horizontal separation lines in these two tables. The ratio R values were averaged in each bin according to the total uncertainties, i.e., with a weight proportional to the inverse of $\sigma_{\text{tot}}^2 = R^2 \times (\sigma_{\text{stat}}^2 + \sigma_{\text{ptp}}^2 + \Delta_{\text{norm}}^2/3 + \Delta_{\text{QED}}^2/3)$. The corresponding averaged Born effective cross sections (σ_{had}^0) and centre-of-mass energy values are displayed in Table 3. The R values found for PEP/PETRA were found to agree with those of an earlier combination [8]. The effective Born hadronic cross section (σ_{th}^0) predicted by ZFITTER [25] is also shown in Table 3.

The ratio and the difference of these measured cross sections and those predicted by ZFITTER are displayed in Fig. 1 as a function of the centre-of-mass energy. When no systematic uncertainties are assigned to the theoretical prediction, the average ratio appears to exceed the prediction by $(0.79 \pm 0.52)\%$, i.e., by 1.5 standard deviations. This excess is, however, about 2.4 standard deviations below the prediction of an additional light sbottom pair production (here with a mass of $6 \text{ GeV}/c^2$), which would amount to about 2% of the total cross section.

The experimental correlations between the different bins, essential for a rigorous statistical treatment of the data, were determined following the lines of Ref. [8]. In practice, a Monte Carlo technique relying on the generation of many gedanken experiments was used to determine the probability density functions of the measured R ratio values listed in Tables 1 and 2.

Table 3

The ratio R and the effective Born hadronic cross section, σ_{had}^0 , from PEP, PETRA, TRISTAN, as a function of the centre-of-mass energy (\sqrt{s}), averaged in ~ 2 GeV-wide centre-of-mass-energy bins. The hadronic cross section prediction, σ_{th}^0 , is also shown. The last column displays the number of measurements used for each entry

\sqrt{s} (GeV)	Ratio R	σ_{had}^0 (pb)	σ_{th}^0 (pb)	N_{pts}
21.995	3.843 ± 0.067	754.1 ± 13.1	763.1	5
25.003	4.047 ± 0.167	616.4 ± 25.4	592.2	3
28.932	3.945 ± 0.045	450.3 ± 5.2	444.4	5
30.570	3.929 ± 0.086	402.2 ± 8.8	399.1	6
34.408	3.996 ± 0.038	323.9 ± 3.1	317.6	12
36.022	3.871 ± 0.102	286.6 ± 7.5	291.0	4
38.237	3.894 ± 0.105	255.9 ± 6.9	260.2	3
41.329	4.083 ± 0.081	230.3 ± 4.6	225.7	7
43.825	4.027 ± 0.051	202.2 ± 2.6	203.7	7
46.038	4.234 ± 0.098	192.9 ± 4.5	187.6	6
53.097	4.527 ± 0.097	155.8 ± 3.3	153.6	12
56.432	4.964 ± 0.087	151.1 ± 2.6	145.4	9
57.867	4.926 ± 0.046	142.7 ± 1.3	143.4	16
60.264	5.456 ± 0.107	145.8 ± 2.9	142.2	9
61.521	5.378 ± 0.156	138.0 ± 4.0	142.8	4

Computer-readable files for these data will be transmitted to the Review of Particle Physics and are available at <http://janot.web.cern.ch/janot/HadronicData/>.

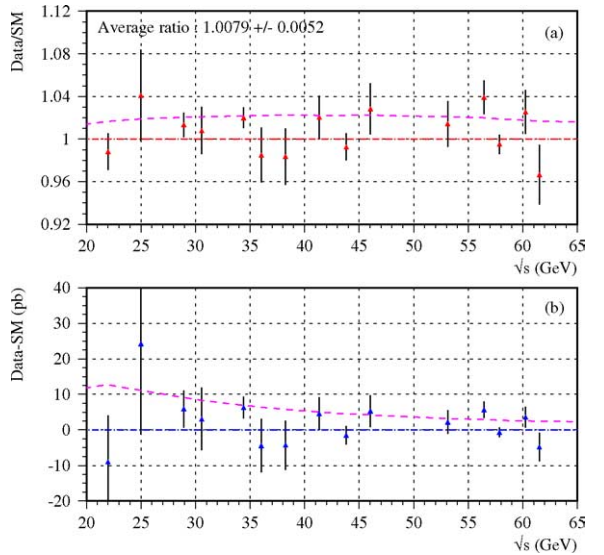


Fig. 1. Ratio (a) and difference (b) of the effective Born hadronic cross section measurements and the ZFITTER prediction as a function of the centre-of-mass energy, for PEP, PETRA and TRISTAN data, rebinned as explained in the text. The dash-dotted line indicates the Standard Model prediction, and the dashed curve the additional contribution of sbottom pair production with $m_{\tilde{b}} = 6 \text{ GeV}/c^2$ and with a vanishing coupling to the Z.

Table 4

The correlations between the ten PEP and PETRA centre-of-mass energy bins (\sqrt{s} in GeV)

\sqrt{s}	21.994	25.003	28.932	30.572	34.409	36.027	38.231	41.325	43.824	46.042
21.994	1.000	0.034	0.003	0.043	0.237	0.060	0.028	0.084	0.227	0.066
25.003	0.034	1.000	0.004	0.053	0.096	0.055	0.012	0.053	0.029	0.041
28.932	0.003	0.004	1.000	0.032	0.017	0.009	0.000	0.003	0.001	0.002
30.572	0.043	0.053	0.032	1.000	0.198	0.105	0.009	0.057	0.030	0.043
34.409	0.237	0.096	0.017	0.198	1.000	0.185	0.032	0.148	0.258	0.113
36.027	0.060	0.055	0.009	0.105	0.185	1.000	0.010	0.096	0.048	0.071
38.231	0.028	0.012	0.000	0.009	0.032	0.010	1.000	0.030	0.054	0.030
41.325	0.084	0.053	0.003	0.057	0.148	0.096	0.030	1.000	0.078	0.098
43.824	0.227	0.029	0.001	0.030	0.258	0.048	0.054	0.078	1.000	0.066
46.042	0.066	0.041	0.002	0.043	0.113	0.071	0.030	0.098	0.066	1.000

Table 5

The correlations between the five TRISTAN centre-of-mass energy bins (\sqrt{s} in GeV)

\sqrt{s}	53.141	56.436	57.863	60.253	61.519
53.141	1.000	0.101	0.014	0.077	0.057
56.436	0.101	1.000	0.017	0.093	0.073
57.863	0.014	0.017	1.000	0.022	0.010
60.253	0.077	0.093	0.022	1.000	0.058
61.519	0.057	0.073	0.010	0.058	1.000

In each gedanken experiment, 108 R values were generated around the measured central value, smeared by (i) a Gaussian distribution with a width equal to the quadratic sum of σ_{stat} and σ_{ptp} ; (ii) a uniform distribution in the $[-\Delta_{\text{norm}}, +\Delta_{\text{norm}}]$ interval, identical for all energy points of a given publication; and (iii) a uniform distribution in the $[-\Delta_{\text{QED}}, +\Delta_{\text{QED}}]$ interval, identical for all 108 measurements.

As above, an average value R_i was determined in each centre-of-mass-energy bin i for each gedanken experiment. This allowed the R_i values of Table 3 and their uncertainties to be confirmed, when averaging over a large number of gedanken experiments. Similarly, the uncertainties of the cross-products $R_i \times R_j$ led to the correlation matrices shown in Tables 4 and 5, for PEP and PETRA on the one hand, and for TRISTAN on the other. The cross-correlations between PEP, PETRA and TRISTAN (induced solely by Δ_{QED}) were found to be smaller than 5×10^{-4} and were therefore neglected in the following.

2.2. The LEP 1 and SLC data

The precise measurements of LEP and SLC and their correlations [21] are summarized in Table 6.

Most of these Z observables would be modified in case of an additional new physics contribution to hadronic Z decays. Let $\varepsilon_{\text{NP}}^{\text{had}}$ be the ratio of this new partial width Γ_{NP} to the total decay width of the Z without this new contribution. As was shown in Ref. [27], the Z total width Γ_Z , the ratio R_ℓ of the hadronic to the leptonic branching fractions, and the peak cross section σ_{had}^0 are modified as follows,

$$\Gamma_Z \rightarrow \Gamma_Z(1 + 1.00\varepsilon_{\text{NP}}^{\text{had}}), \quad [\Gamma_Z + \Gamma_{\text{NP}}], \quad (3)$$

$$R_\ell \rightarrow R_\ell(1 + 1.43\varepsilon_{\text{NP}}^{\text{had}}), \quad [(\Gamma_{\text{had}} + \Gamma_{\text{NP}})/\Gamma_\ell], \quad (4)$$

$$\sigma_{\text{had}}^0 \rightarrow \sigma_{\text{had}}^0(1 - 0.57\varepsilon_{\text{NP}}^{\text{had}}), \quad \left[\frac{12\pi}{m_Z^2} \frac{\Gamma_{ee}(\Gamma_{\text{had}} + \Gamma_{\text{NP}})}{(\Gamma_Z + \Gamma_{\text{NP}})^2} \right]. \quad (5)$$

In Ref. [27], the new hadronic decay channel considered was flavour-democratic. The individual branching fractions into the different quark flavours were therefore not modified by this new contribution. In the case of a sbottom pair production with hadronic R-parity-violating decays into light quarks exclusively, the ratio of the $b\bar{b}$ branching ratio to the hadronic branching ratio, R_b , is also modified according to

$$R_b \rightarrow R_b(1 - 1.43\varepsilon_{\text{NP}}^{\text{had}}), \quad [\Gamma_{b\bar{b}}/(\Gamma_{\text{had}} + \Gamma_{\text{NP}})], \quad (6)$$

while (g_V/g_A) remains untouched.

These observables would also be modified by the virtual corrections arising from the new physics responsible for the additional hadronic contribution. As in Ref. [27], the value of $\varepsilon_{\text{NP}}^{\text{had}}$ was fitted to the measurement of the five observables together with the generic contribution of these virtual effects. The result

Table 6

Precise LEP and SLC measurements of the Z lineshape parameters (Γ_Z , R_ℓ , σ_{had}), of g_V/g_A and of R_b , together with their correlation matrix. The last two measurements have been taken here as uncorrelated with the first three [26]. The Standard Model prediction formula are given in Ref. [27]

Observable	Measurement	Correlation matrix				
Γ_Z	2495.2 ± 2.3 MeV	1.000				
R_ℓ	20.767 ± 0.025	+0.004	1.000			
σ_{had}	41.541 ± 0.037 nb	-0.297	+0.183	1.000		
g_V/g_A	0.07408 ± 0.00068	0.000	0.000	0.000	1.000	
R_b	0.21638 ± 0.00066	0.000	0.000	0.000	0.000	1.000

is

$$\varepsilon_{\text{NP}}^{\text{had}} = (-0.56 \pm 0.80) \times 10^{-3}, \quad (7)$$

which corresponds to an additional hadronic contribution of

$$\sigma_{\text{had}}^{\text{NP}}(m_Z) = -24 \pm 36 \text{ pb}. \quad (8)$$

It allows a 95% C.L. upper limit of 56 pb to be set on the cross section, at the Z peak, of any additional hadronic contribution to the Z decays into light quarks only. The resonant contribution of the sbottom pair production cross section [28] with $m_{\tilde{b}} = 6 \text{ GeV}/c^2$ is shown in Fig. 2 as a function of the mixing angle $\cos \theta_{\text{mix}}$ between the two sbottom states \tilde{b}_L and \tilde{b}_R , superpartners of the left-handed and right-handed bottom quarks, respectively. For $\cos \theta_{\text{mix}} \simeq 0.39$, the coupling between the Z and the lighter sbottom vanishes.

For $m_{\tilde{b}} = 6 \text{ GeV}/c^2$, the Z data allow all values of $\cos \theta_{\text{mix}}$ below 0.22 and above 0.52 to be excluded at the 95% confidence level. These data are therefore incompatible with a light sbottom pair production, unless the coupling to the Z is negligibly small.

2.3. The LEP 2 data

The preliminary LEP 2 hadronic cross section data were taken from Ref. [21]. The measured cross sections σ_{had} and the Standard Model predictions σ_{th} are summarized in Table 7. These data are displayed in Fig. 3 and the correlation matrix is given in Table 8. When no systematic uncertainties are assigned to the theoretical prediction, the average ratio appears to exceed the prediction by $(1.5 \pm 0.9)\%$, i.e., by 1.7 standard deviations. This excess, although not significant, is compatible with, and actually slightly

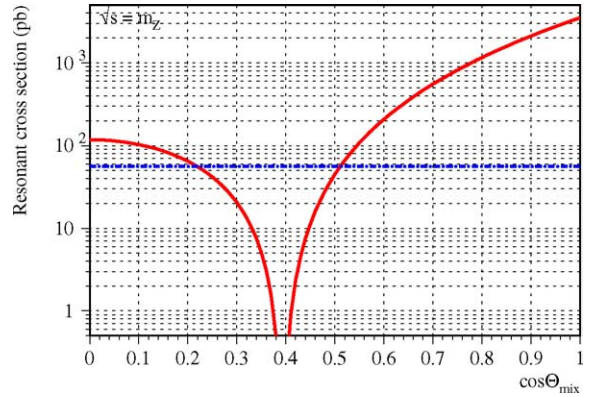


Fig. 2. The resonant contribution of the sbottom pair production cross section with $m_{\tilde{b}} = 6 \text{ GeV}/c^2$, at $\sqrt{s} = m_Z$, as a function of $\cos \theta_{\text{mix}}$ (full curve). The dash-dotted line indicates the 95% C.L. upper limit on this cross section when the sbottom decays into light quarks exclusively.

Table 7

The hadronic cross section, σ_{had} , measured at the twelve LEP 2 centre-of-mass energies, and the predictions in the Standard Model, σ_{th} . These data are still preliminary

\sqrt{s} (GeV)	σ_{had} (pb)	σ_{th} (pb)
130	82.1 ± 2.2	82.8
136	66.7 ± 2.0	66.6
161	37.0 ± 1.1	35.2
172	29.23 ± 0.99	28.74
183	24.59 ± 0.42	24.20
189	22.47 ± 0.24	22.16
192	22.05 ± 0.53	21.24
196	20.53 ± 0.34	20.13
200	19.25 ± 0.32	19.09
202	19.07 ± 0.44	18.57
205	18.17 ± 0.31	17.81
207	17.49 ± 0.26	17.42

larger than an additional light sbottom pair production with $\cos \theta_{\text{mix}} = 0.39$. The latter would amount to about

Table 8

The correlations between the twelve LEP 2 centre-of-mass energy bins (\sqrt{s} in GeV)

\sqrt{s}	130	136	161	172	183	189	192	196	200	202	205	207
130	1.000	0.071	0.080	0.072	0.114	0.146	0.077	0.105	0.120	0.086	0.117	0.138
136	0.071	1.000	0.075	0.067	0.106	0.135	0.071	0.097	0.110	0.079	0.109	0.128
161	0.080	0.075	1.000	0.077	0.120	0.153	0.080	0.110	0.125	0.090	0.124	0.145
172	0.072	0.067	0.077	1.000	0.108	0.137	0.072	0.099	0.112	0.081	0.111	0.130
183	0.114	0.106	0.120	0.108	1.000	0.223	0.117	0.158	0.182	0.129	0.176	0.208
189	0.146	0.135	0.153	0.137	0.223	1.000	0.151	0.206	0.235	0.168	0.226	0.268
192	0.077	0.071	0.080	0.072	0.117	0.151	1.000	0.109	0.126	0.090	0.118	0.138
196	0.105	0.097	0.110	0.099	0.158	0.206	0.109	1.000	0.169	0.122	0.162	0.190
200	0.120	0.110	0.125	0.112	0.182	0.235	0.126	0.169	1.000	0.140	0.184	0.215
202	0.086	0.079	0.090	0.081	0.129	0.168	0.090	0.122	0.140	1.000	0.132	0.153
205	0.117	0.109	0.124	0.111	0.176	0.226	0.118	0.162	0.184	0.132	1.000	0.213
207	0.138	0.128	0.145	0.130	0.208	0.268	0.138	0.190	0.215	0.153	0.213	1.000

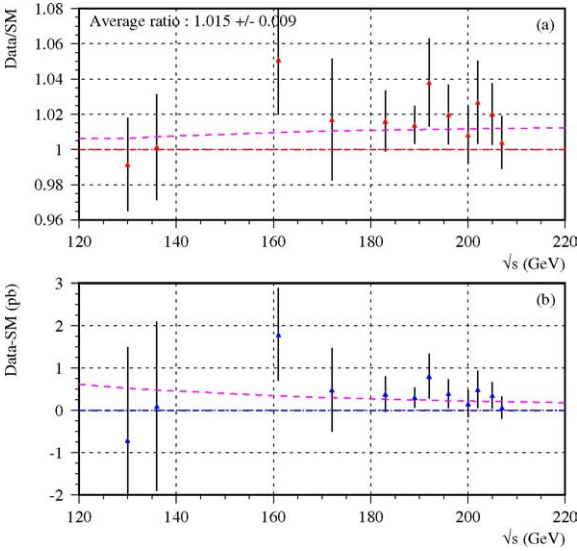


Fig. 3. Ratio (a) and difference (b) of the hadronic cross section measurements and the Standard Model prediction as a function of the centre-of-mass energy, for the LEP 2 data. The dash-dotted line indicates the Standard Model prediction, and the dashed curve the additional contribution of sbottom pair production with $m_{\tilde{b}} = 6 \text{ GeV}/c^2$ and $\cos\theta_{\text{mix}} = 0.39$.

1% of the total cross section in this centre-of-mass energy range.

3. Global fit

When no systematic uncertainties are assigned to the Standard Model prediction, the data can be combined in a global negative log-likelihood $\mathcal{L}(\cos\theta_{\text{mix}}, \alpha)$

as follows,

$$\mathcal{L}(\cos\theta_{\text{mix}}, \alpha) = \frac{1}{2} \sum_{i,j=1}^N \Delta_i S_{ij}^{-1} \Delta_j \quad \text{with}$$

$$\Delta_i = \sigma_{\text{had},i} - [\sigma_{\text{th},i} + \alpha \sigma_{\text{NP},i}(m_{\tilde{b}}, \cos\theta_{\text{mix}})], \quad (9)$$

where S is the covariance matrix of the N ($= 28$) measurements of PEP, PETRA, TRISTAN, LEP 1, SLC and LEP 2 as compiled in Section 2, θ_{mix} is the mixing angle in the sbottom sector and α is an arbitrary normalization constant of the sbottom pair production cross section, $\sigma_{\text{NP},i}$. The likelihood is then minimized with respect to $\cos\theta_{\text{mix}}$ and to α to find the best fit to the data. A fitted value of α compatible with unity and incompatible with 0 would be the sign of new physics, while a value compatible with 0, but incompatible with 1, would allow this new physics to be excluded with a certain level of confidence. (This same technique can be applied for any kind of new physics leading to hadronic final states in e^+e^- collisions.)

For $\alpha = 1$ and $m_{\tilde{b}} = 6 \text{ GeV}/c^2$, the negative log-likelihood is displayed in Fig. 4(a) as a function of $\cos\theta_{\text{mix}}$. Not surprisingly, the Z peak data (Section 2.2) constrain the coupling of the sbottom to the Z to be vanishingly small, $\cos\theta_{\text{mix}} = 0.39 \pm 0.07$.

The value of the mixing angle was therefore fixed to $\cos\theta_{\text{mix}} = 0.39$. The combined negative log-likelihood and those for PEP/PETRA, TRISTAN and LEP 2 data are shown in Fig. 4(b) as a function of α . (For LEP 1 and SLC, the likelihood does not depend on α , because of the vanishing sbottom cross section for $\cos\theta_{\text{mix}} = 0.39$.) The values of α for which the different negative

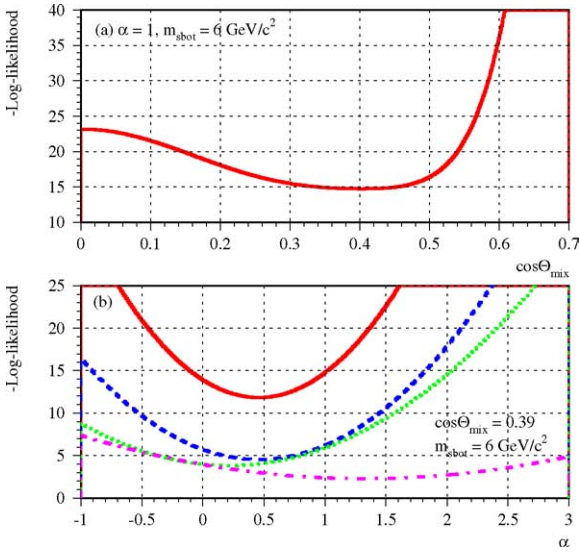


Fig. 4. The negative log-likelihood with $m_{\tilde{b}} = 6 \text{ GeV}/c^2$ (a) as a function of $\cos \theta_{\text{mix}}$ for $\alpha = 1$; and (b) as a function of α with $\cos \theta_{\text{mix}} = 0.39$ for the combined data (full curve), PEP/PETRA (dashed curve), TRISTAN (dotted curve) and LEP 2 (dash-dotted curve).

Table 9

The values α_{min} for which the negative log-likelihood is minimized in PEP/PETRA, TRISTAN and LEP 2 data, and in the combination, together with the 68% confidence intervals and the 95% C.L. upper limits, α_{95} , for $\cos \theta_{\text{mix}} = 0.39$ and $m_{\tilde{b}} = 6 \text{ GeV}/c^2$

Data	α_{min}	α_{95}
PEP/PETRA	0.45 ± 0.30	0.94
TRISTAN	0.21 ± 0.39	0.85
LEP 2	1.32 ± 0.74	2.52
All	0.45 ± 0.23	0.82

log-likelihood functions are minimized are indicated in Table 9, together with the corresponding 68% confidence intervals and the 95% C.L. upper limits on α . (This one-sided upper limit is the α value for which the negative log-likelihood increases by $1.64^2/2$ with respect to the minimum.)

As was already alluded to in Section 2.1, the lower energy data do not favour the sbottom hypothesis ($\alpha = 1$). They are, instead, compatible with the Standard Model ($\alpha = 0$) within one standard deviation or thereabout. A slight excess in the LEP 2 data, at the 1.7σ level (Section 2.3), translates as such to the combined result. The latter, however, excludes the sbottom hypothesis with $m_{\tilde{b}} = 6 \text{ GeV}/c^2$ at more than

95% C.L., when no systematic uncertainty is assigned to the Standard Model prediction.

The main sources of uncertainty for the theoretical prediction of the $e^+e^- \rightarrow q\bar{q}$ cross section are (i) the knowledge and the running of the strong coupling constant α_S ; (ii) the running of the electromagnetic coupling constant α_{QED} ; and (iii) the theoretical accuracy of the prediction from the ZFITTER program. As in Ref. [27], the values and the uncertainties of the strong and electromagnetic coupling constants were taken to be

$$\alpha_S(m_Z) = 0.1183 \pm 0.0020 \text{ [29]} \quad \text{and} \quad \alpha(m_Z)^{-1} = 128.95 \pm 0.05 \text{ [21]}, \quad (10)$$

leading to uncertainties in the hadronic cross section prediction of 0.15 and 0.08%, respectively. The missing higher orders in ZFITTER are estimated to contribute another 0.1%. These numbers add quadratically to a total systematic uncertainty η_{th} of the order of 0.2%, in agreement with the estimate of Ref. [21] ($\eta_{\text{th}} = 0.26\%$) for LEP 2 data.

If this common systematic uncertainty is assumed to have a Gaussian probability density function, the negative log-likelihood can be modified as follows, to account for the full correlation between all centre-of-mass energies:

$$\mathcal{L} = \frac{1}{2} \sum_{i,j=1}^N \Delta'_i S_{ij}^{-1} \Delta'_j + \frac{\rho_{\text{th}}^2}{2\eta_{\text{th}}^2} \quad \text{with} \quad \Delta'_i = \sigma_{\text{had},i} - [(1 + \rho_{\text{th}})\sigma_{\text{th},i} + \alpha\sigma_{\text{NP},i}], \quad (11)$$

where ρ_{th} is the actual theoretical bias of the Standard Model prediction, to be fitted from the data.

It is reasonable, however, to take into account the non-Gaussian nature of uncertainties of theoretical origin. For example, the missing higher orders in ZFITTER may turn into a bias of -0.1 , 0 or 0.1% with an equal probability. (In fact, the least likely value is certainly 0%, as missing orders are expected to contribute a finite amount to the cross section.) Similarly, the uncertainty on the absolute value of $\alpha_S(m_Z)$ is dominated by theory, and cannot be considered as Gaussian. It is therefore probably more adequate to assume a probability density function as displayed in Fig. 5, i.e., flat between $-\eta_{\text{th}}$ and $+\eta_{\text{th}}$, and with a Gaussian shape outside this interval.

Table 10

The values α_{\min} for which the combined negative log-likelihood is minimized for Gaussian and non-Gaussian uncertainties, together with the 68% confidence intervals and the 95% C.L. upper limits, α_{95} , for $\cos\theta_{\text{mix}} = 0.39$ and $m_{\tilde{b}} = 6 \text{ GeV}/c^2$. The fit results for PEP/PETRA, TRISTAN and LEP 2 (α_{PETRA} , α_{TRISTAN} and $\alpha_{\text{LEP 2}}$) are also given

Uncertainties	α_{\min}	α_{95}	α_{PETRA}	α_{TRISTAN}	$\alpha_{\text{LEP 2}}$
Gaussian	0.45 ± 0.24	0.85	0.45 ± 0.35	0.16 ± 0.47	1.68 ± 1.02
Non-Gaussian	$0.34^{+0.42}_{-0.24}$	0.92	$0.59^{+0.31}_{-0.57}$	$0.06^{+0.69}_{-0.48}$	1.87 ± 1.02

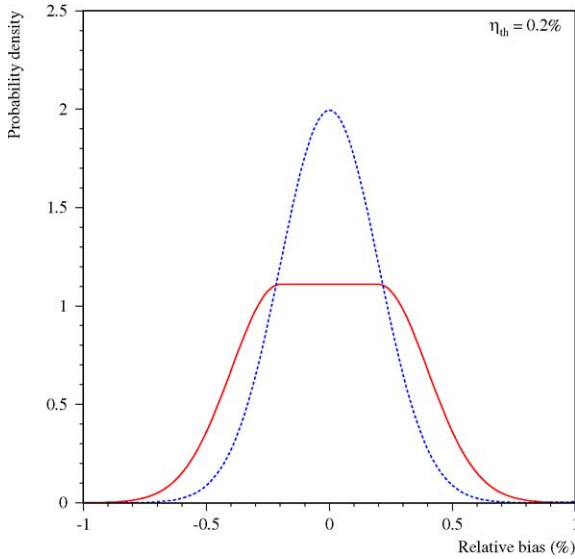


Fig. 5. Probability density function for the conventional (Gaussian) systematic uncertainty treatment (dashed curve) and suggested here instead (full curve) to account for the non-Gaussian nature of theory uncertainties, with $\eta_{\text{th}} = 0.2\%$.

The likelihood was therefore further modified by changing the $\rho_{\text{th}}^2/2\eta_{\text{th}}^2$ term to

$$(\rho_{\text{th}} + \eta_{\text{th}})^2/2\eta_{\text{th}}^2 \quad \text{if } \rho_{\text{th}} < -\eta_{\text{th}}, \quad (12)$$

$$0 \quad \text{if } -\eta_{\text{th}} < \rho_{\text{th}} < \eta_{\text{th}}, \quad (13)$$

$$(\rho_{\text{th}} - \eta_{\text{th}})^2/2\eta_{\text{th}}^2 \quad \text{if } \rho_{\text{th}} > \eta_{\text{th}}. \quad (14)$$

This negative log-likelihood was then minimized with respect to the theoretical bias ρ_{th} , for each value of α , with Gaussian and non-Gaussian uncertainties. The result is displayed in Fig. 6 in the two configurations as a function of α , for $\cos\theta_{\text{mix}} = 0.39$ and $m_{\tilde{b}} = 6 \text{ GeV}/c^2$. The values of α for which the negative log-likelihood is minimized are indicated in Table 10, together with the corresponding 68% confidence intervals and the 95% C.L. upper limits on α .

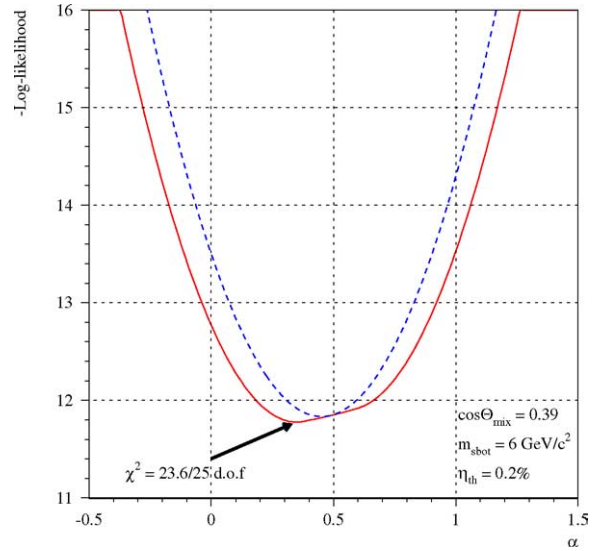


Fig. 6. The combined negative log-likelihood curves with theoretical systematic uncertainties included, assumed to be Gaussian (dashed curve) or non-Gaussian (full curve), as a function of α for $\cos\theta_{\text{mix}} = 0.39$ and $m_{\tilde{b}} = 6 \text{ GeV}/c^2$.

It can be seen that the upper limit on α depends very little on the way the common systematic uncertainties are dealt with. The most conservative approach is chosen here to derive the final results.

4. Results

The same procedure was repeated by varying the sbottom mass from 0 to 12 GeV/c^2 . For each mass, the 95% C.L. upper limit on α was determined as explained above. A sbottom with a given mass is excluded if this upper limit is smaller than unity. Fig. 7 shows the 95% C.L. upper limit on α for $\cos\theta_{\text{mix}} = 0.39$ as a function of the sbottom mass, with Gaussian and non-Gaussian uncertainties. (In the latter configuration, the non-Gaussian nature of the

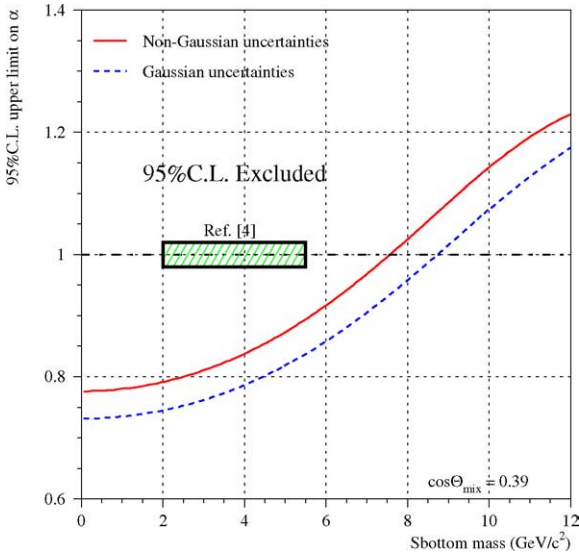


Fig. 7. The 95% C.L. upper limit on α as a function of the sbottom mass, with non-Gaussian (full curve) and Gaussian (dashed curve) common systematic uncertainties. Also shown are the predictions of the model of Ref. [4], now excluded by this analysis.

likelihood was taken into account in the determination of the limit.) Sbottom masses below $7.5 \text{ GeV}/c^2$ are excluded at the 95% confidence level.

Because $\cos\theta_{\text{mix}}$ is very much constrained by the Z peak data, the upper limit on α is expected to be smaller than that shown in Fig. 7 for any other value of the mixing angle. As a check, the procedure was repeated again by varying $\cos\theta_{\text{mix}}$ from 0 to 1, with non-Gaussian uncertainties. The resulting sbottom mass lower limit is shown in Fig. 8 as a function of $\cos\theta_{\text{mix}}$, and is indeed at least $7.5 \text{ GeV}/c^2$ over the whole range. (The region excluded by LEP 2 data at large values of $\cos\theta_{\text{mix}}$ is probably over-optimistic, as four-jet events—expected from such heavy sbottom pair as well as W pair production—are rejected from the $q\bar{q}$ event samples selected above the WW threshold.)

It is worth mentioning that the presence of a light sbottom would slow down the running of α_S with the centre-of-mass energy. (It would be even more so with an additional light gluino.) Starting from the value accurately measured in τ decays [30] (the only measurement not affected by a sbottom heavier than $2 \text{ GeV}/c^2$ and lighter than $5.5 \text{ GeV}/c^2$, and corresponding to $\alpha_S(Z) = 0.121 \pm 0.003$ in the

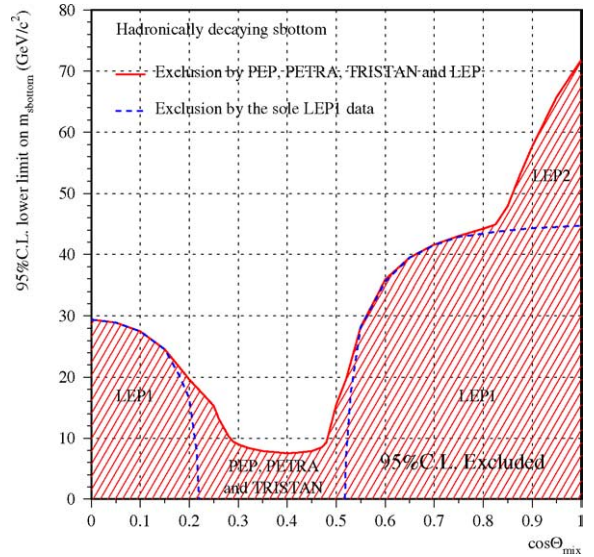


Fig. 8. Absolute 95% C.L. lower limit on $m_{\tilde{b}}$ as a function of $\cos\theta_{\text{mix}}$, for hadronically decaying sbottoms. The hatched area is excluded at 95% C.L. The dashed line shows the exclusion achieved with the sole Z peak data.

Standard Model), this slower running would lead to values of α_S larger than assumed in this Letter, at all centre-of-mass energies. The total new physics contribution (from the direct sbottom production and the increase of α_S) would further increase the effect on the total hadronic cross section expected at PEP, PETRA, TRISTAN, SLC and LEP. The $7.5 \text{ GeV}/c^2$ lower limit on the sbottom mass is therefore probably very conservative.

5. Conclusion

The $e^+e^- \rightarrow \text{hadron}$ cross section data collected well above the $b\bar{b}$ resonances have been compiled and analysed to search for an anomalous production of hadronic events. Altogether, the PEP, PETRA, TRISTAN, LEP 1, SLC and LEP 2 data allow a light sbottom decaying hadronically to be excluded at 95% C.L. for any mixing angle, if its mass is below $7.5 \text{ GeV}/c^2$. When combined with the result of Ref. [5] in which a stable sbottom with mass below $92 \text{ GeV}/c^2$ is excluded, this analysis definitely invalidates the model of Ref. [4] with a $12\text{--}16 \text{ GeV}/c^2$ gluino and a $2\text{--}5.5 \text{ GeV}/c^2$ sbottom.

Note added

This work has been primarily motivated by the “apparent excess” reported in Ref. [31]. With the collaborative help of the author, the excess was found to be an artifact of duplicated, missing and over-corrected data in the computer-readable files of the Review of Particle Physics [22,23] augmented by an incorrect interpretation of the Z peak data in Ref. [31]. The aforementioned computer-readable files are being updated to include the work described in this Letter.

Acknowledgements

I am grateful to German Rodrigo, Sabine Kraml and the CERN Journal Club on Phenomenology for having suggested this analysis to me, and to Günther Dissertori, Vladimir Ezhela, Michelangelo Mangano, Ramon Miquel, Michael Schmitt, Daniel Treille and Oleg Zenin for interesting discussions. Many thanks are due to Bolek Pietrzyk, Helmut Burkhardt, Gerardo Ganis and Brigitte Bloch for their help with ZFITTER and other Monte Carlo programs, and for many enlightening exchanges. Finally, I am indebted to my Physics Letters referees for many constructive suggestions.

References

- [1] DØ Collaboration, Phys. Rev. Lett. 74 (1995) 3548; DØ Collaboration, Phys. Rev. Lett. 85 (2000) 5068; DØ Collaboration, Phys. Lett. B 487 (2000) 264.
- [2] CDF Collaboration, Phys. Rev. Lett. 71 (1993) 500; CDF Collaboration, Phys. Rev. Lett. 71 (1993) 2396; CDF Collaboration, Phys. Rev. D 50 (1994) 4252; CDF Collaboration, Phys. Rev. Lett. 75 (1995) 1451; CDF Collaboration, Phys. Rev. D 65 (2002) 052005; CDF Collaboration, Phys. Rev. D 66 (2002) 032002.
- [3] M. Cacciari, et al., hep-ph/0312132, CERN-TH/2003-298 (2003), and references therein.
- [4] E.L. Berger, et al., Phys. Rev. Lett. 86 (2001) 4231.
- [5] ALEPH Collaboration, Eur. Phys. J. C 31 (2003) 327.
- [6] MARK II Collaboration, Phys. Rev. D 43 (1990) 34.
- [7] MAC Collaboration, Phys. Rev. D 31 (1985) 1537.
- [8] CELLO Collaboration, Phys. Lett. B 183 (1987) 400.
- [9] JADE Collaboration, Phys. Rep. 148 (1987) 67.
- [10] MARK J Collaboration, Phys. Rev. D 34 (1986) 681.
- [11] TASSO Collaboration, Z. Phys. C 22 (1984) 307.
- [12] TASSO Collaboration, Z. Phys. C 47 (1990) 187.
- [13] PLUTO Collaboration, Phys. Rep. 83 (1983) 151.
- [14] AMY Collaboration, Phys. Rev. D 42 (1990) 1339.
- [15] TOPAZ Collaboration, Phys. Lett. B 234 (1990) 525.
- [16] TOPAZ Collaboration, Phys. Lett. B 304 (1993) 373.
- [17] TOPAZ Collaboration, Phys. Lett. B 347 (1995) 171.
- [18] VENUS Collaboration, Phys. Lett. B 198 (1987) 570.
- [19] VENUS Collaboration, Phys. Lett. B 234 (1990) 297; VENUS Collaboration, Phys. Lett. B 246 (1990) 382.
- [20] VENUS Collaboration, Phys. Lett. B 447 (1999) 167.
- [21] LEP and LEPEWWG Collaborations, hep-ex/0312023, and references therein.
- [22] O.V. Zenin, et al., hep-ph/0110176, computer-readable files can be found at <http://wwwppds.ihep.su:8001/comphp.html>.
- [23] Particle Data Group, Review of Particle Physics, Phys. Rev. D 66 (2002) 259, computer-readable files can be found at http://pdg.lbl.gov/2002/contents_plots.html.
- [24] M.R. Whalley, J. Phys. G: Nucl. Part. Phys. 29 (2003) A1.
- [25] D. Bardin, et al., Comput. Phys. Commun. 133 (2001) 229. The version 6.36 of ZFITTER was used here, with FOT2 set to -1 and CONV set to 0, to compute the effective Born hadronic cross section corrected for QED effects, σ_{had}^0 , with the most recent vacuum polarization determination from <http://www-zeuthen.desy.de/~fjeger/hadr5n.f>.
- [26] B. Pietrzyk, private communication.
- [27] P. Janot, Phys. Lett. B 564 (2003) 183.
- [28] H. Eberl, A. Bartl, W. Majerotto, Phys. Lett. B 349 (1995) 463.
- [29] The central α_S value is taken from the latest world average in S. Bethke, hep-ex/0211012; And the theory uncertainty from Particle Data Group, Review of Particle Physics, Phys. Rev. D 66 (2002) 89.
- [30] ALEPH Collaboration, Phys. Lett. B 307 (1993) 209; OPAL Collaboration, Eur. Phys. J. C 7 (1999) 571.
- [31] M. Schmitt, hep-ex/0401034.